

## Perpendicular magnetic anisotropy in $\text{Mn}_2\text{VIn}$ (001) films: An *ab initio* study

Muthui Zipporah,<sup>1,2,3,a,b</sup> Musembi Robinson,<sup>1,a</sup> Mwabora Julius,<sup>1,a</sup>  
and Kashyap Arti<sup>2,a,c</sup>

<sup>1</sup>Department of Physics, University of Nairobi, P.O.Box 30197, 00100 Nairobi, Kenya

<sup>2</sup>School of Basic Sciences, Indian Institute of Technology, Mandi, Himachal Pradesh 175005, India

<sup>3</sup>Chuka University, P.O. Box 109, 60400 Chuka, Kenya

(Presented 8 November 2017; received 1 October 2017; accepted 13 October 2017; published online 7 December 2017)

First principles study of the magnetic anisotropy of  $\text{Mn}_2\text{VIn}$  (001) films show perpendicular magnetic anisotropy (PMA), which increases as a function of the thickness of the film. Density functional theory (DFT) as implemented in the Vienna *Ab initio* simulation package (VASP) is employed here to perform a comprehensive theoretical investigation of the structural, electronic and magnetic properties of the  $\text{Mn}_2\text{VIn}$ (001) films of varying thickness. Our calculations were performed on fully relaxed structures, with five to seventeen mono layers (ML). The degree of spin polarization is higher in the (001)  $\text{Mn}_2\text{VIn}$  thin films as compared to the bulk in contrast to what is usually the case and as in  $\text{Mn}_2\text{VAl}$ , which is isoelectronic to  $\text{Mn}_2\text{VIn}$  as well as  $\text{InCo}_2\text{VIn}$  (001) films studied for comparison. Tetragonal distortions are found in all the systems after relaxation. The distortion in the  $\text{Mn}_2\text{VIn}$  system persists even for the 17ML thin film, resulting in PMA in the  $\text{Mn}_2\text{VIn}$  system. This significant finding has potential to contribute to spin transfer torque (STT) and magnetic random access memory MRAM applications, as materials with PMA derived from volume magnetocrystalline anisotropy are being proposed as ideal magnetic electrodes. © 2017 Author(s). All article content, except where otherwise noted, is licensed under a Creative Commons Attribution (CC BY) license (<http://creativecommons.org/licenses/by/4.0/>). <https://doi.org/10.1063/1.5007211>

### INTRODUCTION

Perpendicular magnetic anisotropy (PMA) greatly enhances the performance of high speed spin-based electronics by offering fast switching with low currents and high thermal stability in conventional computing applications and magnetic tunneling junction (MTJ) memory elements.<sup>1-3</sup> In the magnetic random access memory (MRAM), a high PMA barrier is needed for the stability of stored information against temperature fluctuations while in the process of reading.

Electrodes used in perpendicular MTJ's (p-MTJ) require a sufficient interfacial PMA, such that their magnetization lies perpendicular to the plane of the MTJ device. This requires the films to be sufficiently thin so that the interfacial PMA overcomes the in-plane shape anisotropy of the magnetic volume of the film. Ultra thin CoFeB electrodes, containing the soft 3d ferromagnets, with an MgO barrier, exhibit high interfacial PMA, but the PMA is too weak for thicknesses  $< \sim 20\text{nm}$ , which are necessary to maintain the moment perpendicular to the film.<sup>2-4</sup>

Magnetic materials that derive their PMA from volume magnetocrystalline anisotropy such as tetragonally distorted Heusler compounds, would be ideal candidates to provide PMA in films of increased thickness, which has already been exhibited in  $\text{Mn}_3\text{Ge}$  films.<sup>3</sup> Epitaxial thin

<sup>a</sup>All the authors contributed equally to this work.

<sup>b</sup>This research was performed while Muthui Z. was at IIT- Mandi, India.

<sup>c</sup>Electronic mail: [arti@iitmandi.ac.in](mailto:arti@iitmandi.ac.in)

films of  $\text{Mn}_2\text{CoGa}$  (001) prepared by DC magnetron co-sputtering on  $\text{MgO}$  (001) substrate were found to have a slight tetragonal distortion resulting from lattice mismatch with the substrate<sup>5</sup> while addition of increasing thickness of  $\text{MnGa}$  in  $\text{Co}_2\text{FeAl}$  increased PMA.<sup>6</sup> The coercivity of  $\text{Pr-Fe-B}$  films in the thickness range from 25 to 1200 nm grown on a Mo under layer initially increased with increasing film thickness.<sup>4</sup> PMA was achieved in annealed  $\text{CoFeB/MgO}$  films within a thickness range of 0.7 nm – 1.2 nm with a maximum value achieved at 0.9 nm. In this study, nonlinearity commonly observed for thin magnetic layers with PMA in their curves was attributed to the thickness dependent magneto elastic coupling.<sup>7</sup> PMA was observed in the  $\text{Co}_2\text{TiSi/GaAs}$  at large thicknesses, as high as 13.5 nm, in which interfacial anisotropy was ruled out as it is not a long range effect and the squareness of the hysteresis curve which indicates PMA was least in the thinnest films.<sup>8</sup>

Heusler compounds like  $\text{Co}_2\text{FeAl}$  have been predicted by first principle investigations to have a high interfacial PMA and a giant electric field assisted modification of the PMA.<sup>2</sup> Additionally,  $\text{Co}_2\text{MnSi}$  Heusler films were reported to have a spin polarization of 60% at low temperatures as well as PMA for the super lattice films prepared using the (111)  $\text{MgO}$  substrate.<sup>9,10</sup>  $\text{Co}_2\text{TiSn}$  films on Cr buffered  $\text{MgO}$  (001) surfaces and  $\text{V}_3\text{Al}$  have been grown by DC magnetron co-sputtering, resulting in well ordered films having the  $\text{L}_{21}$  structure.<sup>11,12</sup>

Manganese based Heusler compound  $\text{Mn}_2\text{VAl}$  has been found to be a half metallic ferrimagnet with the Fermi level in the minority spin band gap, having atomic moments of  $1.5\mu_B$  and  $-0.9\mu_B$  on Mn and V in agreement with experiment.<sup>13</sup> We focus on  $\text{Mn}_2\text{VIn}$  which is isoelectronic to  $\text{Mn}_2\text{VAl}$  and carry out a systematic first principle investigation of the properties of its (001) thin films and compare them to the closely related  $\text{Co}_2\text{VIn}$  and  $\text{Mn}_2\text{VAl}$  thin films of the same orientation.

## COMPUTATIONAL DETAILS

Electronic structure calculations were carried out within the framework of Density functional theory (DFT) with spin orbit coupling (SOC), as implemented in the Vienna ab initio simulation package (VASP) using the projector augmented wave (PAW) method employing the Perdew-Burke-Ernzerhof parameterization of the generalized gradient approximation (PBE-GGA) to treat the exchange and correlation in the systems. We used a plane wave basis set with a kinetic energy cut off of 430 eV and a Monkhorst-Pack grid of  $9 \times 9 \times 1$   $\mathbf{k}$  points for both the total energy calculations as well as the magnetic anisotropy energy calculations, which gave a good balance between accuracy and computational time. The optimized bulk lattice parameters for  $\text{Mn}_2\text{VIn}$ ,  $\text{Mn}_2\text{VAl}$ , and  $\text{Co}_2\text{VIn}$  of, 6.25 Å, 5.80 Å and 6 Å, respectively, were used to model the supercells of varying thicknesses having between five to thirteen mono layers (ML) and a vacuum of 12.5 Å. Thin films with (001) orientation having YZ termination grown in the z direction of thickness ranging between 5.99 Å to 21.17 Å, containing 20, 36 and 52 ions, respectively, and corresponding to one unit cell to three unit cell thickness were modeled. Additionally, 8 and 17ML  $\text{Mn}_2\text{VIn}$  films of thickness 14.82 and 26.1 Å, having 32 and 68 ions were grown to probe the properties of  $\text{Mn}_2\text{VIn}$  further. While all the films had the standard YZ termination, the film of thickness 14.82 Å consisted of 8ML's and therefore had an XX termination as can be seen in Fig. 1, in which the 9ML supercell is shown with the alternating YZ and XX layers. The geometry optimization was carried out by relaxation of the atomic positions as well as the shape of the unit cell until the Hellman-Feynman force on each atom was less than 10 meV/Å, before performing the electronic structure calculations as well as magnetic anisotropy energy calculations. The magnetic anisotropy energy (MAE) was calculated from the difference between the total energies of the system when the magnetization is in the (001) plane and normal to the (001) plane, respectively i.e.,  $E_{(\text{MAE})} = E(100) - E(001)$ .

## RESULTS AND DISCUSSIONS

In this section, a detailed account of the structure of the supercells is given, alongside a detailed comparison with the respective bulk structures from which they are grown from. Their electronic and magnetic properties are then reported.

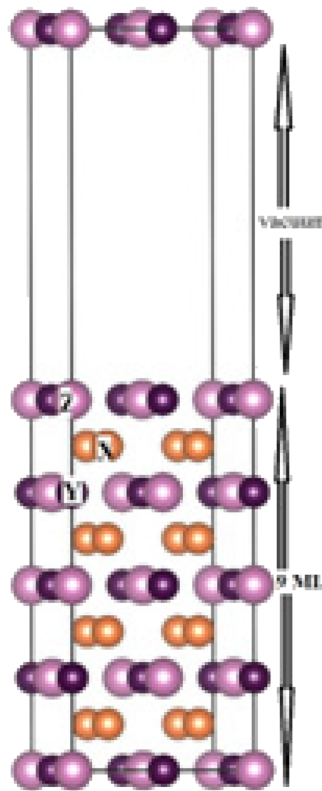


FIG. 1. 9ML Supercell for  $X_2YZ$  (001) films.

### Structural properties

Relaxation of the internal degrees, as well as shape of the (001)  $Mn_2VIn$  supercells, composed of alternating  $VIn$  and  $MnMn$  planes, resulted in an increase in the  $c$  parameter and a reduction in the  $a$  and  $b$  parameters. This reduced the forces on the surface ions arising from the broken symmetry and reduced coordination, as compared to the bulk system. An analysis of the changes arising from the relaxation of the supercells revealed an interesting non-linear trend in the (001)  $Mn_2VIn$  supercells, whereby, an initial increase in the tetragonal distortion, which we denote in this work as the percentage change in  $c/a$  ratio,  $\% \Delta c/a$  shown in Table I, was noted for the 8 and 9ML supercells as compared to the 5ML one, but decreased subsequently for the 13 and 17ML supercells as expected, as dimensions become more bulk like. However, the 8ML film has a  $MnMn$  termination and was studied additionally together with the 17ML supercell, so as to probe the anomaly observed in the 9ML supercell. A comparison with  $\% \Delta c/a$  of the  $Mn_2VAl$  and  $Co_2VIn$  supercells, revealed that in these systems, the distortion was linear, whereby it decreased with increased supercell thickness and that it was highest in the Indium based systems.

In addition to analyzing the degree of distortion using  $\% \Delta c/a$ , we also monitored the change in volume of the supercells on relaxation, occasioned by the changes in the lattice parameters on relaxation of the supercells. A non-linear trend was noted for  $Mn_2VIn$ , with the 9ML supercell experiencing the least change in volume on relaxation as compared to the 8 & 13ML supercells, contrary to what is the case in both  $Mn_2VAl$  and  $Co_2VIn$  supercells. We attribute this conservation of the volume on relaxation of the 9ML supercell to the triggering of an intrinsic tetragonal distortion at this thickness that brings about the anomaly, such that the change in volume is not only due to relaxation so as to reduce the forces on the surface atoms, but also due to an energetically favorable structural distortion inherent to the crystal structure. The volume of the relaxed 17ML supercell film is approximately equal to that of the bulk. In the case of  $Mn_2VAl$  and  $Co_2VIn$  supercells however, as the film thickness increased to the nanometer scale, less change in volume resulted on relaxation

TABLE I. Magnetic moments for,  $\text{Mn}_2\text{VIn}$ ,  $\text{Co}_2\text{VIn}$  and  $\text{Mn}_2\text{VAl}$  films of different thickness as well as for each atom in the system.

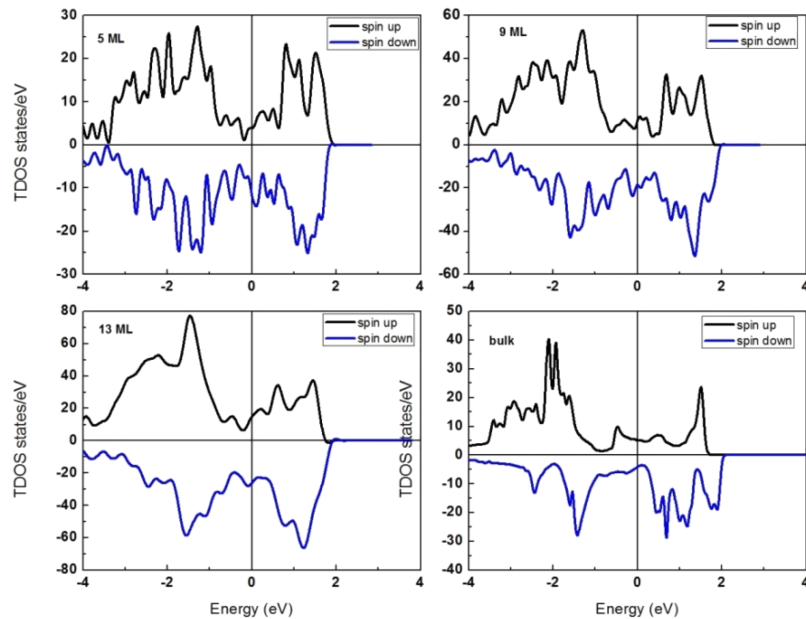
$\text{X}_2\text{VIn}(\text{Co, Mn})$	System	X(Co, Mn $\mu_B$ )	V ( $\mu_B$ )	In ( $\mu_B$ )	Total ( $\mu_B/\text{f.u.}$ )	% $\Delta c/a$	$E_{\text{MAE}}(\text{meV})$
$\text{Mn}_2\text{VIn}$	5ML	1.590	-1.370	-0.010	1.800	23.00	2.089
	8ML	2.660	-1.750	-0.069	3.501	24.57	3.680
	9ML	2.264	-1.682	-0.039	2.807	25.00	6.790
	13ML	2.330	-1.740	-0.060	2.860	21.67	
	17ML	2.875	-2.038	-0.058	3.654	6.50	
	bulk	3.009	-1.979	-0.059	3.980	-	
	5 ML	-0.018	0.134	0.0003	0.098	50.00	87.760
$\text{Co}_2\text{VIn}$	9 ML	0.099	0.262	-0.005	0.455	34.50	0.146
	13 ML	0.923	0.230	-0.034	2.042	10.00	
	bulk	0.928	0.192	-0.047	2.001	-	
	5 ML	-0.684	0.681	0.010	-0.677	6.00	0.545
$\text{Mn}_2\text{VAl}$	9 ML	1.065	-0.808	-0.016	1.306	2.50	0.461
	13 ML	1.168	-0.831	-0.018	1.487	1.67	
	bulk	1.426	-0.895	-0.021	1.936	-	

of the supercells, such that the 13ML supercell had almost the same volume as the bulk system with  $\text{Mn}_2\text{VAl}$  having bulk-like dimensions at thicknesses as low as  $\sim 12 \text{ \AA}$ .

These results point to the importance of the atomic radii of the Z element in stabilizing the structure of the unit cell in which case In being larger than Al causes changes in the dimensions of the unit cell to be more pronounced on relaxation.

### Electronic properties

A pseudo gap is seen in the  $\text{Mn}_2\text{VIn}$  thin films up to a thickness of 13ML's and the spin polarization decreases with film thickness with values of 55.32 %, 30.10 % and 33.42 % for the 5, 9 and 13ML's respectively as shown in Fig. 2. as well as that of the  $\text{Mn}_2\text{VIn}$  bulk system which has a very low spin polarization, with no half metallic gap. The reduced symmetry in the supercells results in change of the lattice parameters after relaxation as explained earlier, leading to a re-hybridization of the 3d states, resulting in increased spin polarization due to the overlap of the 3d orbitals. The Fermi energy

FIG. 2. Total density of states (TDOS) for for 5 ML, 9 ML, 13 ML thick  $\text{Mn}_2\text{VIn}$  films and for the bulk structure.

is slightly above the spin up gap in the 13ML thick  $\text{Mn}_2\text{VIn}$  film of thickness  $21.17\text{\AA}$ . The spin polarization would increase to 71.23 % on a slight contraction of the unit cell, such that the Fermi level lies within the pseudogap, as would happen due to epitaxial stress and such effects have been studied for  $\text{Mn}_2\text{VAl}$  and  $\text{NiMnSb}$ , in which the position of the Fermi level shifted on contraction and expansion of the lattice resulting in increased and reduced hybridization between the  $d$  states respectively.<sup>14,15</sup>

In the case of  $\text{Mn}_2\text{VAl}$  and  $\text{Co}_2\text{VIn}$ , whose bulk structures unlike that of  $\text{Mn}_2\text{VIn}$  are half metallic, as shown in Fig. 3 for  $\text{Mn}_2\text{VAl}$ , surface states are found in the minority spin gap of the thin films due to the reduced symmetry which leads to a re-hybridization among the  $d$  orbitals. In the  $\text{VIn(Al)}$  termination, the V surface atoms lose half their Co(Mn) neighbors compared to the bulk structure, raising the Co(Mn)  $d_{3z^2-r^2}$  states through re-hybridization up to the Fermi level resulting in partially filled surface states as explained for  $\text{Co}_2\text{MnSi}$ .<sup>8</sup> The  $\text{In(Al)}$   $sp$  states contribute to bonding far below the Fermi level while at the Fermi level, only the  $3d$  metal states are present. The spin polarization of the 5, 9 and 13ML  $\text{Co}_2\text{VIn}$  thin films is 38.11%, 63.08% and 65.40% while for the 5, 9 and 13ML thick  $\text{Mn}_2\text{VAl}$  thin films it is 39.27%, 50.54 % and 79.62 % respectively. The spin polarization increases and becomes more bulk like, with the emergence of the half metallic gap as the film thickness increases.

### Magnetic properties

The 5ML  $\text{Mn}_2\text{VIn}$  film has a total magnetic moment of  $1.800 \mu_B$ , very close to the expected  $2\mu_B$  for  $\text{Mn}_2\text{VIn}$ , if half metallic according to the Slater-Pauling rule as seen in Table I. We attribute this observation to the overlapping of the  $3d$  orbitals at the reduced lattice constant, which does not take place in the bulk structure, in which the Mn localized magnetic moment is  $\sim 3 \mu_B$ , a value it's known to have if no hybridization occurs. The magnetic moments then increase with film thickness, with the exception of the 8ML thick film with a MnMn termination which breaks the trend in the value of magnetic moments, as expected due to the symmetry breaking arising from reduced V neighbors. For  $\text{Co}_2\text{VIn}$  and  $\text{Mn}_2\text{VAl}$ , the magnetic moments are lowest for the thinner films and a general increase in the magnetic moments is noted as film thickness increases as shown in Table I.

The general trend is that the thickest films studied have similar total magnetic moments as well as individual atomic magnetic moments as the corresponding bulk systems. For the thin films, the loss of neighbors resulting in breaking of the symmetry causes a re-hybridization hence changing

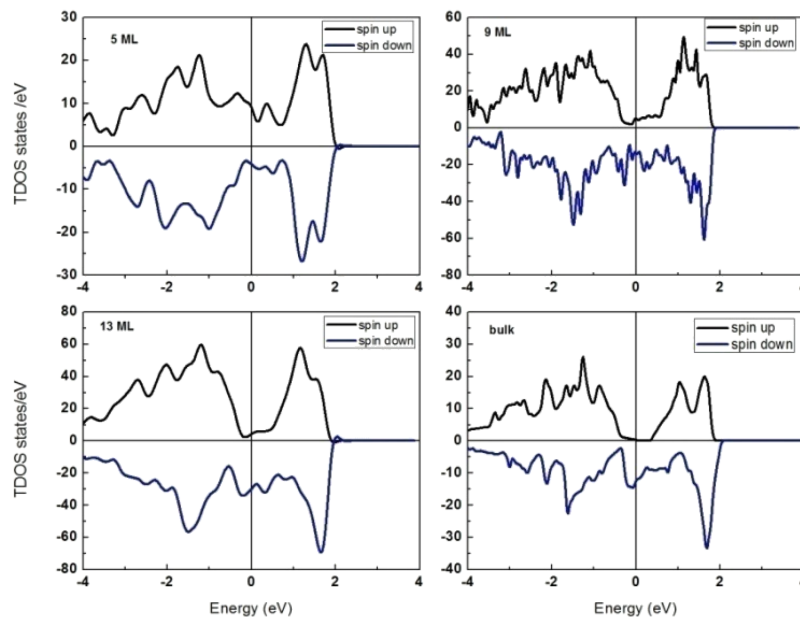


FIG. 3. Total density of states (TDOS) for 5 ML, 9 ML, 13 ML thick  $\text{Mn}_2\text{VAl}$  films and for the bulk structure.

the magnetic moments and changing the spin polarization at the Fermi level.<sup>9</sup> While  $\text{Co}_2\text{VIn}$  is generally ferromagnetic due to the exchange interaction between Co and V,  $\text{Mn}_2\text{VAl}$  and  $\text{Mn}_2\text{VIn}$  are ferrimagnetic and would therefore create smaller external magnetic fields in devices, leading to smaller energy losses.<sup>16</sup>

Of greater technological importance, is the alignment of the magnetization along the tetragonal axis resulting in PMA in the thin films. The trend is collated in Table I as  $E_{\text{MAE}}$  for the 5 and 9ML films in each case, as well as for the 8ML  $\text{Mn}_2\text{VIn}$  film. In  $\text{Mn}_2\text{VIn}$ , the magnetic anisotropy energy ( $E_{\text{MAE}}$ ) increases with film thickness. We attribute this observation to structural distortion in these films and the balance with the film volume, rather than to spin orbit coupling as the orbital moments are too low.

$E_{\text{MAE}}$  for  $\text{Mn}_2\text{VAl}$  is very low for both the 5 and 9ML thickness films, where the tetragonal distortion on relaxation and orbital moments are not sufficient to cause a preferential alignment of the spin moments. It is highest for the  $\text{Co}_2\text{VIn}$  5ML film, in which the tetragonal distortion results in higher surface anisotropy and decreases appreciably in the 9ML thin film.

In  $\text{Mn}_2\text{VIn}$ , the symmetry breaking caused by the higher tetragonal distortion in the thicker films align the spin moments perpendicular to the plane of the film, resulting in increasing PMA with film thickness. The surface magnetism has been shown to be highly dependent on the film volume as is expected for ultra thin films containing a few atomic layers at low temperatures. The exchange coupling in the films is the same as in the bulk, except for the 5ML films, which leads to size effects overriding surface effects and film thickness becoming a significant factor.

## CONCLUSIONS

We have revealed by first principles, two Heusler systems,  $\text{Co}_2\text{VIn}$ , with conventional magnetocrystalline anisotropy only present for very thin films and  $\text{Mn}_2\text{VIn}$ , which exhibits volume anisotropy arising from the distorted structure, which enforces out of plane magnetization. This result is similar to one in which  $\text{Mn}_2\text{CuSb}$  and  $\text{Rh}_2\text{CoSb}$  displayed the same effect and their structures were tetragonally distorted while their parent Heusler compounds are cubic and do not exhibit anisotropy as well as  $\text{Mn}_3\text{Ge}$  films, which have been shown to exhibit giant PMA.<sup>3</sup> The experimental realization of these properties will contribute significantly in spintronics device applications.

## ACKNOWLEDGMENTS

Muthui Z. acknowledges the assistance of OWSD fellowship, IIT-Mandi, India and DAAD for a Ph.D scholarship at the University of Nairobi.

- <sup>1</sup> J. Winterlik *et al.*, "Design scheme of new tetragonal Heusler compounds for spin-transfer torque applications and its experimental realization," *Adv. Mater. Deerfield Beach Fla* **24**(47), 6283–6287 (2012).
- <sup>2</sup> Z. Bai *et al.*, "Magnetocrystalline anisotropy and its electric-field-assisted switching of Heusler-compound-based perpendicular magnetic tunnel junctions," *New J. Phys.* **16**(10), 103033 (2014).
- <sup>3</sup> J. Jeong, Y. Ferrante, S. V. Faleev, M. G. Samant, C. Felser, and S. S. P. Parkin, "Termination layer compensated tunnelling magnetoresistance in ferrimagnetic Heusler compounds with high perpendicular magnetic anisotropy," *Nat. Commun.* **7** (2016).
- <sup>4</sup> F. Yang, W. Liu, W. B. Cui, J. N. Feng, Y. Q. Zhang, and Z. D. Zhang, "Thickness dependence of the magnetic properties of high-coercive Pr-Fe-B thin films with perpendicular magnetic anisotropy," *Phys. B Condens. Matter* **403**(19–20), 3631–3634 (2008).
- <sup>5</sup> M. Meinert *et al.*, "Itinerant and localized magnetic moments in ferrimagnetic  $\text{Mn}_2\text{CoGa}$  thin films probed by x-ray magnetic linear dichroism: Experiment and ab initio theory," *Phys. Rev. B* **84**(13), 132405 (2011).
- <sup>6</sup> Q. L. Ma, X. M. Zhang, T. Miyazaki, and S. Mizukami, "Artificially engineered Heusler ferrimagnetic superlattice exhibiting perpendicular magnetic anisotropy," *Sci. Rep.* **5** (2015).
- <sup>7</sup> P. G. Gowtham, G. M. Stiehl, D. C. Ralph, and R. A. Buhrman, "Thickness-dependent magnetoelasticity and its effects on perpendicular magnetic anisotropy in  $\text{TaCoFeBIMgO}$  thin films," *Phys. Rev. B* **93**(2) (2016).
- <sup>8</sup> M. T. Dau, B. Jenichen, and J. Herfort, "Perpendicular magnetic anisotropy in the Heusler alloy  $\text{Co}_2\text{TiSi/GaAs}(001)$  hybrid structure," *AIP Adv.* **5**(5), 57130 (2015).
- <sup>9</sup> S. J. Hashemifar, P. Kratzer, and M. Scheffler, "Preserving the half-metallicity at the Heusler alloy  $\text{Co}_2\text{MnSi}(001)$  surface: A density functional theory study," *Phys. Rev. Lett.* **94**(9), 96402 (2005).
- <sup>10</sup> N. Matsushita, Y. Takamura, Y. Fujino, Y. Sonobe, and S. Nakagawa, "Magnetic anisotropy of  $[\text{Co}_2\text{MnSi/Pd}]_n$  superlattice films prepared on  $\text{MgO}(001)$ , (110), and (111) substrates," *Appl. Phys. Lett.* **106**(6), 62403 (2015).
- <sup>11</sup> M. Meinert *et al.*, "Electronic structure of fully epitaxial  $\text{Co}_2\text{TiSn}$  thin films," *Phys. Rev. B* **83**(6) (2011).

- <sup>12</sup> M. Tas, E. Sasioglu, C. Friedrich, S. Blugel, and I. Galanakis, "Design of L21-type antiferromagnetic semiconducting full-Heusler compounds: A first principles DFT + GW study," *J. Appl. Phys.* **121**(5), 53903 (2017).
- <sup>13</sup> E. Sasioglu, L. M. Sandratskii, and P. Bruno, "First-principles study of exchange interactions and Curie temperatures of half-metallic ferrimagnetic full Heusler alloys Mn<sub>2</sub>VZ (Z=Al, Ge)," [ArXivcond-Mat0504679](#), Apr. 2005.
- <sup>14</sup> I. Galanakis and P. Mavropoulos, "Spin-polarization and electronic properties of half-metallic Heusler alloys calculated from first principles," *J. Phys. Condens. Matter* **19**(31), 315213 (2007).
- <sup>15</sup> E. Şaşıoğlu, L. M. Sandratskii, P. Bruno, and I. Galanakis, "Exchange interactions and temperature dependence of magnetization in half-metallic Heusler alloys," *Phys. Rev. B* **72**(18), 184415, 2005.
- <sup>16</sup> M. Kawakami, Y. Yoshida, T. Nakamichi, S. Ishida, and H. Enokiya, "Magnetic properties of the Heusler alloy Mn<sub>2</sub>VAl," *J. Phys. Soc. Jpn.* **50**(4), 1041–1042 (1981).